Iraqi National Journal of Earth Science

www.earth.mosuliournals.com

The Effect of Satellite Image Fusion on the Classification Process by Using Multiple Sensors

Nehad H. Al-salmany [1*], Taghreed Abdalhameed Naji [2]

[1,2] Department of Physics, College of Education for Pure Science Ibn-Al-Haitham, University of Baghdad, Baghdad, Iraq.

Article information

Received: 16- Sep -2023

Revised: 02- Dec -2023

Accepted: 22- Feb -2024

Available online: 01- Jan – 2025

Keywords:
Landsat 9
Sentinel 2
Land cover
pan-sharpening
classification

Correspondence:
Name: Nehad H .Al-salmany

Email: nohad.hameed1104a@ihcoedu.uobaghdad.edu.iq

ABSTRACT

Accurate land use and land cover (LU/LC) classification is essential for various geospatial applications, which demand high spatial and spectral resolution imagery. This study investigates the efficacy of pan-sharpening and hybrid data fusion techniques to enhance Landsat 9 and Sentinel 2A imagery for LU/LC classification. The study aims to compare the classification accuracy of different datasets using multiple classifiers: Support Vector Machines (SVM) with various kernels, Maximum Likelihood (ML), Artificial Neural Networks (ANN), Mahalanobis distance, and Minimum Distance. Datasets encompassed the Landsat (30 m) imagery, Landsat pan-sharpened to (15 m) and (10 m), Sentinel 2 pan-sharpened to (10 m), and the hybrid datasets that combined the un-overlapping bands from both satellites at (10 m). The results show a significant improvement in classification accuracy: from 82.28% for Landsat 30m to 89.91% for Landsat 10m and 91.55% for the hybrid dataset using the linear SVM. The hybrid dataset outperformed the individual Landsat and Sentinel 2 pan-sharpened imagery, especially for spectrally overlapped features, demonstrating the value of fusing the information from multiple sensors. SVM classifier with the linear kernel are emerged as the most accurate and robust classifier. This study concludes that pan-sharpening and hybrid data fusion effectively enhance LU/LC classification accuracy. The SVM classifier with the linear kernel is identified as a suitable choice for this task, offering insights valuable for applications in diverse fields.

DOI: 10.33899/earth.2024.143380.1145,

تأثير دمج الصور الفضائية على عملية التصنيف باستخدام أجهزة الاستشعار المتعددة

نهاد حميد السلماني [1*] ، تغريد عبد الحميد ناجي [2]

[1, 2] قسم الفيزياء، كلية التربية للعلوم الصرفة ابن الهيثم، جامعة بغداد، بغداد، العراق.

معلومات الارشفة

تاريخ الاستلام: 16- سبتمبر -2023

تاريخ المراجعة: 02- ديسمبر -2023

تاريخ القبول: 22- فبراير -2024

تاريخ النشر الالكتروني: 01- يناير -2025

الكلمات المفتاحية:

لاندسات 9

سينتنال 2

الغطاء الارضي

الشحذ الشامل

تصنيف

المراسلة:

الاسم: نهاد حميد السلماني

Email: nohad.hameed1104a@ihcoedu.uobaghdad.edu.iq

الملخص

يعد التصنيف الدقيق لاستخدام الأراضي والغطاء الأرضي أمرًا ضروريًا لمختلف التطبيقات الجغرافية المكانية. الأمر الذي يتطلب صورًا ذات دقة مكانية وطيفية عالية. تتناول هذه الدراسة مدى فعالية تقنيات الشحذ الشامل للبيانات ودمج البيانات الهجينة لتحسين صور لاندسات9 وسينتنال2 لتصنيف استخدام الأراضي والغطاء الأرضي. هدفت الدراسة الى مقارنة دقة التصنيف لمجموعات البيانات المختلفة باستخدام مصنفات متعددة: أجهزة المتجهات الداعمة (SVM) ذات النوى المختلفة، والاحتمال الأقصى (ML)، والشبكات العصبية الاصطناعية (ANN)، ومسافة المهالانوبيس، والحد الأدنى للمسافة. تضمنت مجموعات البيانات صور لاندسات (30 م)، ولاندسات المشحوذة إلى (15 م) و (10 م)، وسينتنال٢ المشحوذة إلى (10 م)، ومجموعات البيانات الهجينة التي جمعت بين النطاقات غير المتداخلة من كلا القمرين بدقة (10م). أشارت النتائج إلى تحسن كبير في دقة التصنيف: من 82.28% لـ لاندسات 30 م إلى 89.91% للاندسات 10 م و91.55% لمجموعة البيانات الهجينة باستخدام SVM الخطي. تفوقت مجموعات البيانات الهجينة على صور لاندسات وسينتنال الفردية المشحوذة في تمييز الاصناف المتداخلة طيفيًا، مما يدل على قيمة دمج المعلومات من أجهزة استشعار متعددة. ظهر مصنف SVM ذو النواة الخطية باعتباره المصنف الأكثر دقة وقوة. خلصت هذه الدراسة إلى أن الشحذ الشامل ودمج البيانات الهجينة هما من التقنيات الفعالة لتعزيز دقة تصنيف استخدام الأراضي والغطاء الأرضي. تم تحديد مصنف SVM مع النواة الخطية كخيار مناسب لهذه المهمة، مما يوفر رؤى قيمة للتطبيقات في مجالات متنوعة.

DOI: 10.33899/earth.2024.143380.1145,

Introduction

Land use and land cover (LU/LC) information is essential for a wide range of geospatial applications including regional administration, urban planning, and environmental management (Liu *et al.*, 2017; Naji, 2018). However, to avoid confusion, it is essential to establish clear distinctions between the terms (LU) and (LC), where LC refers to the biotic and abiotic elements on the Earth's surface, encompassing categories such as forests, grasslands, water bodies, urban areas, and more (Giri, 2012). On the other hand, LU relates to the activities or purposes for which humans utilize the land (Lambin and Geist, 2008). Accurate mapping of LC/LU is imperative to obtain pertinent information for these applications (Waldner *et al.*, 2015). Earth observation utilizes remote sensing, a critical data acquisition and analysis tool. Remote sensing data's continuous availability has made it an initial pillar for understanding Earth's dynamics. However, converting raw data into meaningful information through image classification is a challenging task (Mountrakis *et al.*, 2011), where the similarities in surface spectral features aggravate the challenge of classifying images based on shared characteristics. End-member extraction algorithms can be used as a powerful tool for classifying images based on shared characteristics, even when the surface spectral features of the different classes are similar (Naji and Hatem, 2017). This field has evolved in tandem with advances in artificial

intelligence and computer vision, with pattern recognition, image classification, and feature extraction forming the foundation of image processing systems (Canty, 2019; Hogland *et al.*, 2013). Traditional methods such as Maximum Likelihood (ML) classification and the Mahalanobis distance algorithm have garnered widespread use. While ML classification hinges on assumptions of normal distribution, equal covariance, and sufficient training samples (Hogland *et al.*, 2013; Pham *et al.*, 2019), the Mahalanobis distance algorithm assumes equal class covariance (Canty, 2019). Artificial neural networks (ANNs) offer a flexible non-linear classification approach, relying less on statistical distribution assumptions (Weng *et al.*, 2007). The Support Vector Machine (SVM), distinguished for its adeptness in handling nonlinear data with limited samples, has emerged as a powerful candidate in pattern recognition (Abduljabbar and Naji, 2020).

The spatial resolution of the data sets highly affects the LU/LC classification accuracy, especially in heterogeneous regions (Murtaza and Romshoo, 2014), the increase in spatial resolution by the mean of image fusion usually increases the classification accuracy (Ghassemian, 2016). Image fusion is combining important details from two or more images into a single image. The fused image resulting from image fusion techniques exceeds the quality and scope of any individual input image (Muhsin and Salih, 2015). Increasing both spectral and spatial resolutions is fundamental for refining mapping accuracy. The fusion of data from diverse sensors demands careful execution to ensure co-registration and uniform pixel size (Townshend *et al.*, 1992). Pan-sharpening, a technique fusing high spatial resolution images with images that have high spectral information, elevates both dimensions, although with potential spatial or spectral distortions (Akula *et al.*, 2012; Amro *et al.*, 2011; Vivone *et al.*, 2014).

The Gram-Schmidt pan-sharpening algorithm is one of the most widely used and robust pan-sharpening algorithms available (Klonus and Ehlers, 2009; Maurer, 2013). This algorithm synthesizes a simulation panchromatic band from the original low-resolution multispectral bands and employs transformations to yield high-resolution pan-sharpened multispectral bands (Laben and Brower, 2000; Majed and Abduljabbar, 2022). The Scheme illustrated in Figure (1) shows the Gram-Schmidt pan-sharpening process.

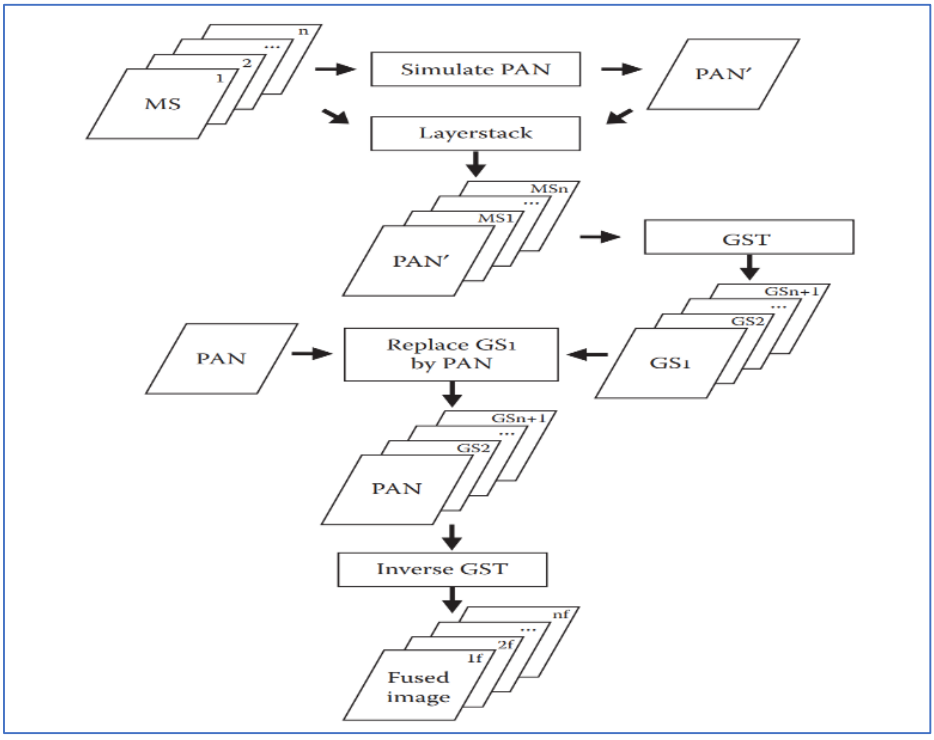

Fig. 1. Gram-Schmidt pan-sharpening process (Pohl and Van Genderen, 2016)

The primary aim of this study is to evaluate the effectiveness of pan-sharpening and data fusion techniques in enhancing the classification accuracy and refining the quality of remotely sensed imagery. This research seeks to demonstrate how these techniques can significantly improve the ability to classify land cover while simultaneously enhancing the overall visual clarity and precision of the acquired imagery. In addition, it is intended to provide critical insights into the careful selection of classifiers and pan-sharpening algorithms, which depend on the peculiarities of the dataset and the broader context of remote sensing applications, where combining techniques stands as a potent approach toward extracting many insights from Earth observation data.

A comprehensive literature review is essential to establish a firm foundation and identify the most relevant research in remote sensing, pan-sharpening, and data fusion techniques and their impact on classification accuracy.

In the sphere of satellite data exploitation, the studies by researchers (Mohammed and Hatem, 2020) used Landsat 8 data to classify land cover in the Diyala River Basin, Iraq. They used a random forest classifier to classify the data into six land cover classes: water, built-up, vegetation, bare land, soil, and salt-affected land.

The researchers (Ali and Muhaimeed, 2016) used Sentinel-2 data to classify land cover in Baghdad City, Iraq. They used a support vector machine (SVM) classifier to classify the data into seven land cover classes: water, built-up, vegetation, bare land, soil, salt-affected land, and rock, the work conducted by researchers (Al-Rubiey, 2017; Hatem *et al.,* 2021; Raheem and Hatem, 2019) used the computation of overall accuracy based on the confusion matrix.

Existing literature presents a variety of methods for integrating data from different satellite sources to improve classification accuracy. The goal is to create fused images with higher spatial resolution. Notably, (Mateen *et al.,* 2023) demonstrated the utilization ability of Sentinel-2 and Landsat 8 (OLI) data. By capitalizing on compatible wavelengths and geographic coordinate systems, the researchers successfully increased the spatial resolution of the two satellites to 10 m for all bands. This improvement resulted in augmented accuracy in supervised classification tasks, particularly obvious in the classification of features like the Billion Trees Tsunami Forest.

The researchers (Mansourmoghaddam *et al.,* 2022) evaluated the Sentinel-2, optical Landsat-8, and their fused images' efficacy in enhancing the land cover (LC) map accuracy for Yazd, Iran using the Gram-Schmidt technique, a primarily spatial fusion of Landsat-8 images with Sentinel-2 images. Then, the Sentinel spectral bands (four 10m bands) were combined with the fused Landsat's spectral bands in a new dataset. Resulting in four datasets (Landsat-8 30-m, Sentinel-2 10-m, spatially fused Landsat image (10 m), and spectral-spatial fused image (Landsat 10 m + Sentinel 10 m), all classified applying the Maximum Likelihood (MLC) method. The results revealed a substantial 10% increase in overall classification accuracy compared to the initial unfused Landsat-8 image.

Similarly, (Sigurdsson *et al.,* 2022) embraced a parallel approach by fusing data from Sentinel-2 (S2) and Landsat 8 (L8) satellites. Their technique incorporated the Sentinel-2 Sharpening (S2Sharp) approach, involving the integration of spectral bands from Landsat 8 and subsequently sharpening all bands to the data's maximum available resolution of 10 m. Their evaluation of this modified method uses both authentic and simulated data. Also, (Muhsin and Foud, 2012) employed four distinct fusion methods to enhance the multispectral imagery captured by the Landsat 7 Thematic Mapper (ETM+) with its three bands (red, green, blue), alongside the panchromatic image obtained via the SPOT satellite.

Absalom and his coauthors (Bouslihim *et al.,* 2022) compared the performance of pan-sharpened Landsat 9 and Sentinel-2 imagery for land-use classification using machine learning classifiers. They found that pan-sharpened Sentinel-2 imagery outperforms pan-sharpened Landsat-9 imagery for land-use classification.

Researchers (Abduljabbar, 2017; Al-Rubiey, 2017; Drakonakis *et al.,* 2022; Hafner *et al.,* 2021) have studied the fusion of data originating from diverse sensors. The fusion process involves the integration of radar wave imagery and visible light imagery through advanced methods, presenting a general perspective on data fusion's potential for comprehensive Earth observation applications.

The researchers (Al-Jasim *et al.,* 2022) showed that the increased difference in spatial resolution between merged images reduces the color quality of the resulting merged image

Materials and Methods

Study site and data sources

Study site

The selected study site for this research is between (3669870 - 3699870) of latitudes, and (427890 - 457890) of longitudes with an area of (900) square kilometers. The predominant feature of the study area is Baghdad City, the capital of Iraq. The city exhibits a high density of urbanization, with limited green regions and bare land areas. The Tigris River runs through the city dividing it into two parts and it merges with the Diyala River in the southern section (Abdullah *et al.,* 2023). The study area includes other geographic features such as smaller tributaries, canals, and artificial lakes. Other parts of the study area predominantly comprise agricultural regions having green areas with palm trees, wheat, barley, fodder crops, and various orchards covering smaller areas. Urbanization in these regions is characterized by low population density. The western part of the study area is Baghdad International Airport. The elevation of the study area above sea level is approximately (31-39) m (Saleh, 2010). The land use pattern in the study area is diverse. There are other land uses, such as industrial zones, commercial districts, and transportation infrastructure**.** Figure (2 a, b, c) shows the original scenes of Landsat 9 and Sentinel 2 projected on the Iraq map, and the clipped study region, respectively.

Data sources

The research utilizes satellite imagery from Landsat 9 OLI/TIRS C2 L2 and Sentinel 2A MSI. The Landsat 9 OLI C2 L2 collection provides global surface reflectance products (Maciel *et al.,* 2023; Rahman and Robson, 2020). The satellite scene data extracted from the original scene identified by LANDSAT_PRODUCT_ID = "LC09_L2SP_168037_20230220_ 20230223_02_T1". The scene center time was recorded at "07:33:58.7530860Z".

The Landsat 9 satellite has two instruments: the Operational Land Imager 2 (OLI-2) and the Thermal Infrared Sensor (TIRS-2). The (OLI-2) consists of 11 channels (dynamic range 14-bit), the first seven channels being multispectral (visible, near-infrared, shortwave infrared) registered at 30 m spatial resolution. The eighth band is the panchromatic, which has a resolution of 15 m. TIRS-2 consists of two thermal infrared channels with a spatial resolution of 100 m (Choate *et al.,* 2022; Masek *et al.,* 2020; Micijevic *et al.,* 2022; Niroumand-Jadidi *et al.,* 2022; Wulder *et al.,* 2022). The panchromatic band is downloaded from LANDSAT_PRODUCT_ID = "LC09_L1TP_168037_20230220_20230221_02_T1" as it was not included in the Level 2 bundles. All the data are collected from the OLI-2 sensor. The band 9 (Cirrus), and TIRS-2 bands are neglected in this work. Landsat data are downloaded from https://earthexplorer.usgs.gov/.

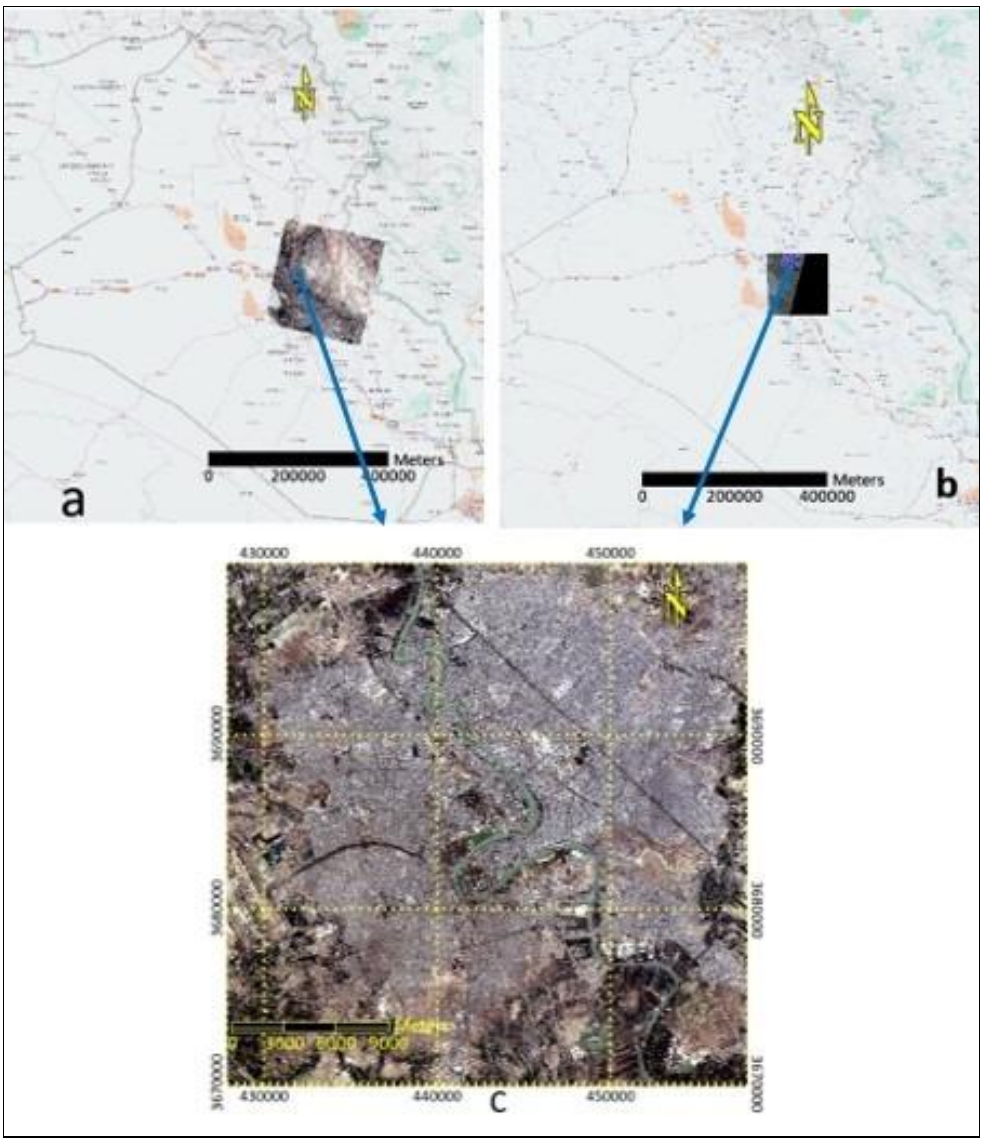

Fig. 2. (a), (b) Iraqi country map with two scenes (Landsat 9, and Sentinel 2A respectively) for the study site, (c) The clipped original Sentinel 2A (B4, B3, and B2) color composite of the study site by ENVI 5.6 program.

Sentinel 2A data are acquired from the European Union's Earth observation program through https://scihub.copernicus.eu/. Sentinel 2A is equipped with the Multispectral Imager (MSI), which consists of 13 channels with various spatial resolutions (10, 20, and 60 m) with wavelengths covering the visible, near-infrared, and shortwave infrared spectrums. However, Sentinel 2 has no panchromatic band (ESA, 2015; Wang *et al.*, 2016). Level-2A (surface reflectance, ortho-images in UTM/WGS84 projection) is available to users under a free and open data policy (Aguilera, 2020; ESA *et al.*, 2020).

The study region is extracted from the original scene with the ID: S2A_MSIL2A_20230220T074941_N0509_R135_T38SMB_20230220T110210.

Both satellites are freely available worldwide and share the same geographic coordinate system making it an excellent opportunity to combine these two types of satellite sensor data (Wang *et al.*, 2017).

Both datasets have undergone geometric correction ensuring accurate spatial representation. Additionally, atmospheric correction has been applied to convert sensor radiance to surface reflectance. These corrections performed by the data providers enhance the reliability of the datasets. However, it’s important to note that the panchromatic band (Band 8) of Landsat 9 is an exception and has not been atmospherically corrected.

Table 1: The available Satellite Scenes Information

Satellite Scene	Spatial Resolution	Date	Local Acquisition Time	Scene Dimensions km^2
Landsat 9_OLI	(30 and15) m	20 February 2023	10:33:58	900
Sentinel 2A	(10, 20 and 60) m	20 February 2023	10:49:41	900

Methodology

The Sentinel-2A dataset and the Landsat 9 imagery are merged using the Gram-Schmidt pan-sharpening technique to increase both the spatial and spectral resolutions.

First, a simulated panchromatic band is created by averaging the four Sentinel-2 bands with a high spatial resolution of 10 m (B2, B3, B4, and B8) (Kaplan and Avdan, 2018).

Then, the spatial resolution of all other Sentinel-2 bands (20 and 60 m) is increased to 10 m using the simulated panchromatic band.

The Landsat panchromatic band (15 m) is used to increase the spatial resolution of the Landsat multispectral (MS) bands to 15 m. These original MS Landsat bands (30 m) are then pan-sharpened again using the simulated panchromatic band to achieve a resolution of 10 m.

Next, both Landsat and Sentinel-2 bands are uniformly resampled to a resolution of 10 m and stacked together based on their wavelengths to produce a new dataset containing all the un-overlapped wavelength bands of the two satellites.

Finally, these combined bands are pan-sharpened using the Gram-Schmidt algorithm to achieve a unified spatial resolution of 10 m resulting in a hybrid dataset that effectively enhances the spectral resolution (Mansourmoghaddam *et al.,* 2022).

Five distinct datasets are selected for the classification process: Landsat 9 (30, 15, 10 m), Sentinel 2A (10 m), and the Hybrid dataset (10 m). Four supervised classification algorithms are used: minimum distance, maximum likelihood, Mahalanobis distance, artificial neural networks, and support vector machine with four kernel functions (linear, polynomial, RBF, and sigmoid). All classification algorithms are executed with their default configurations by the ENVI 5.6 software.

The classification accuracy is assessed based on the overall accuracy (*OA*) (Eq.1) calculations collected from the confusion matrix and training set (ROI). Overall accuracy represents the total percentage of correctly classified pixels (Ahmad and Quegan, 2012).

$$OA = \frac{\text{Total number of correctly classified pixels}}{\text{Total number of pixels}} \times 100\% \text{ ----------(Eq. 1).}$$

To select the training set (ROI-1) for performing the classification process, while (ROI-2) is reserved for the evaluation of classification accuracy, the following steps are carried out:

1- The hybrid satellite dataset is used to identify the different land cover classes in the study area.

2- High-resolution images from Google Earth and Esri are used to cross-reference and validate the land cover classes, especially in areas where the satellite imagery is unclear.

3- Field data are collected to discriminate between uncertain or changeable features, such as agricultural areas and construction sites.

4- The training sets are collected using the pixel-based method, with single-pixel or multi-pixel blocks used depending on the dimensions of the features.

5- Trial and error are used to improve the separability of the classes.

6- Several band combinations are used to designate uncertain features.

7- To compare the classification results between different datasets and algorithms, the same training set is used and re-projected on all datasets.

The flowchart in Figure (3) illustrates the steps of multi-sensor satellite image fusion and the classification methods used in the study.

The resampling process and band math operation are performed using the SNAP 9.0.0 software. All other steps are performed using ENVI 5.6 software.

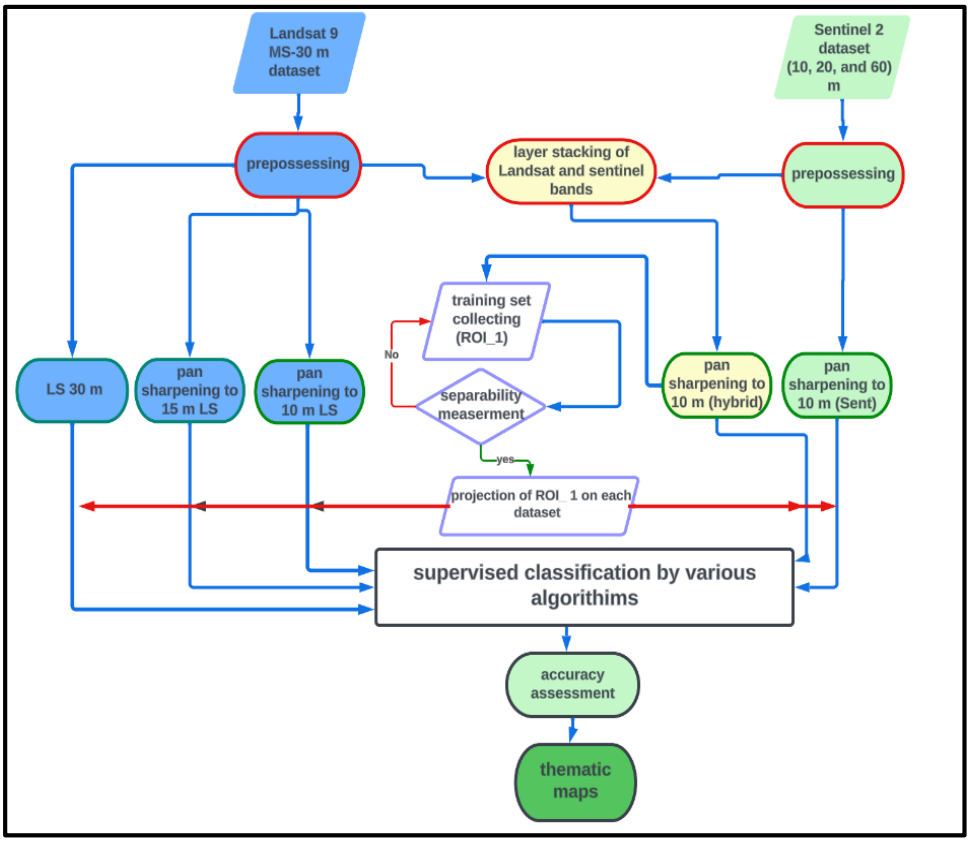

Fig. 3. Flowchart of the proposed method

Results

The supervised classification of the Landsat 30 m dataset shows the lowest overall accuracy among all the used datasets. However, it performs well in classifying spectrally distinct and space-wide features like agricultural areas, barren lands, and large water bodies due to its high radiometric resolution. It struggles to extract features with small geometric dimensions, such as sub-roads and roads partially shadowed by buildings and trees, because they are below the sensor's spatial resolution. The low spatial resolution leads to a decrease in the overall accuracies of this dataset, and this is consistent with the results of researchers (Majed and Abduljabbar, 2022; Roth *et al.*, 2015; Toure *et al.*, 2018).

The neural networks classifier achieved the highest overall accuracy of 82.86%. Support vector machines also performed well with an accuracy of 82.28%, particularly when using the linear kernel. In contrast, the Mahalanobis classifier had the lowest accuracy at 74.125%. Thematic maps displaying the results from various classifiers can be observed in Figure (4) representing this dataset captured by Landsat with a 30-meter resolution.

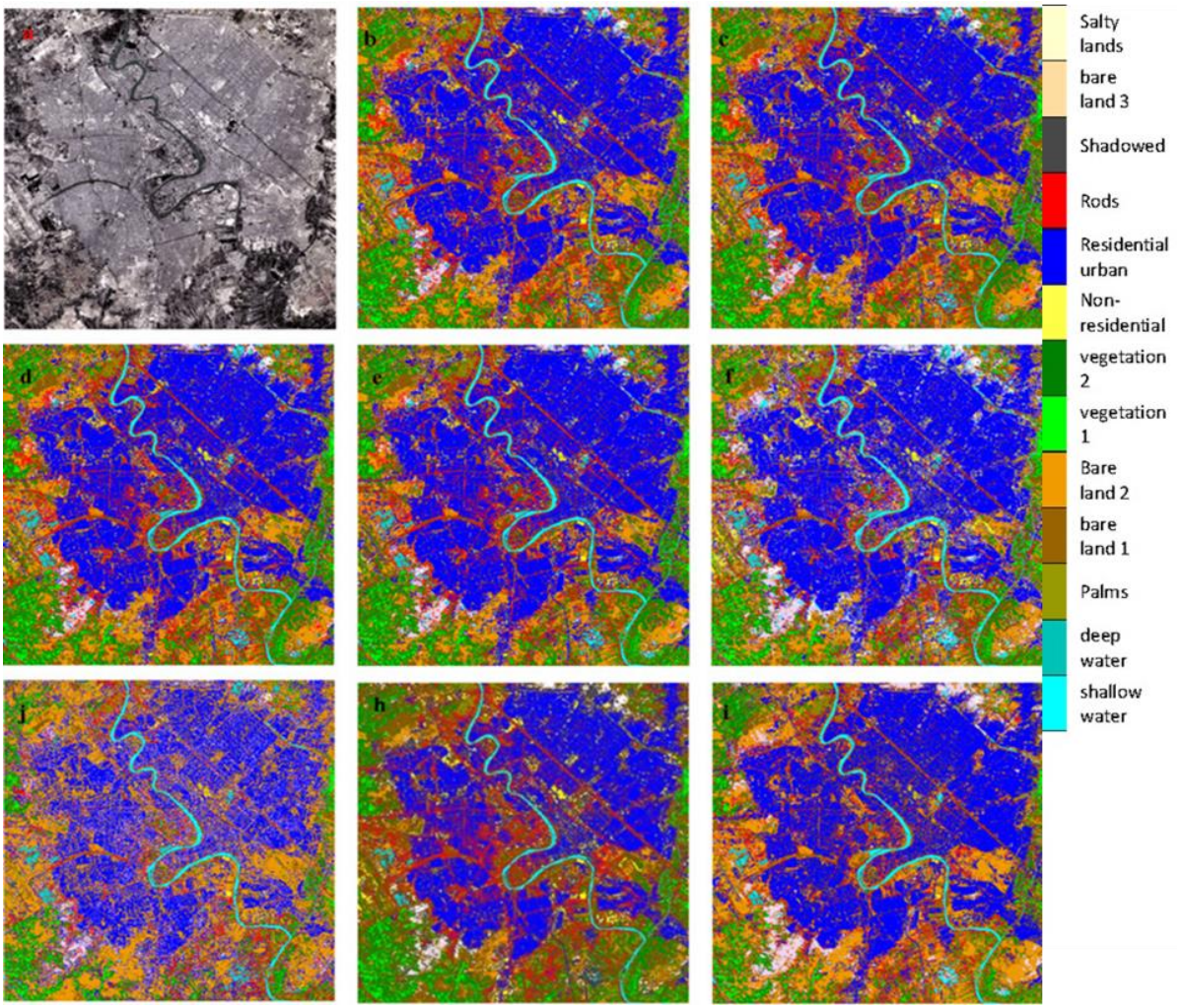

Fig. 4. Classification results of Landsat 30 m dataset; (a) Original image, (b) SVM (Sigmoid), (c) SVM (RBF), (d) SVM (Poly), (e) SVM (Linear), (f) ANN, (j) Minimum distance, (h), ML, and (i) Mahalanobis.

The classification results of the second dataset, LS (15 m) are presented in Figure (5). In this case, the spectral resolution remains unchanged, while the spatial resolution increases from 30 m to 15 m. This boost in spatial resolution leads to a noticeable improvement in overall accuracy (OA) for all classifiers except for the ANN classifier, which shows a slight decrease in OA. Among the classifiers, the SVM classifier with the linear kernel exhibits the highest increase in OA achieving 87.26% with a gain of 4.98%. Notably, several classes demonstrate significant enhancements in producer's accuracies, including bare land 2, salty lands, deep water, and bare land 3, with improvements of 10%, 9%, 8%, and 6% respectively. However, certain classes such as shadowed and bare lands 1 experience reductions in producer's accuracy, with decreases of 6% and 2.5% respectively. Despite these reductions, the overall trend demonstrates substantial improvements in OA and producer's accuracies due to the increased spatial resolution.

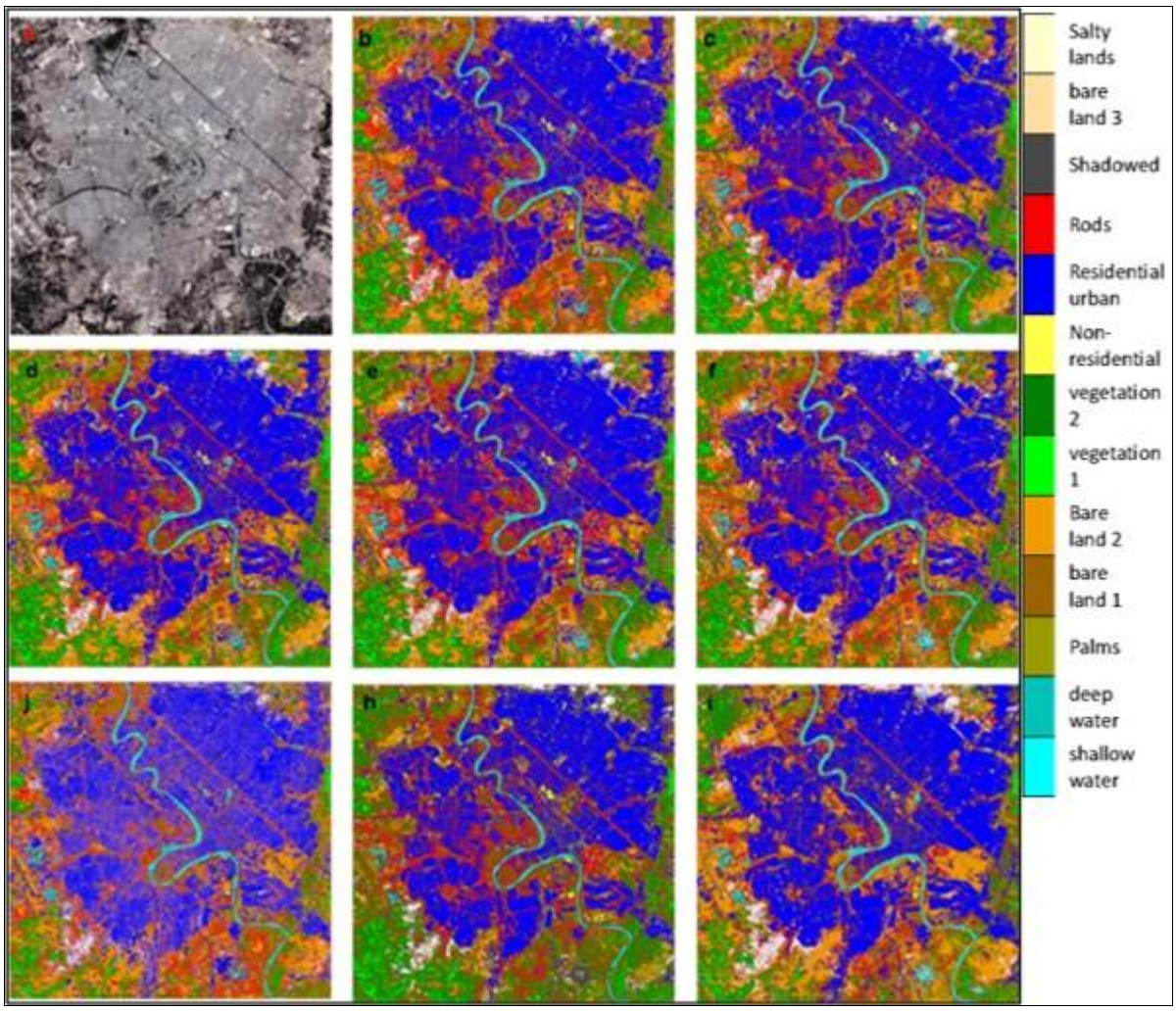

Fig. 5. Classification results of Landsat 15 m dataset; (a) Original image, (b) SVM (Sigmoid), (c) SVM (RBF), (d) SVM (Poly), (e) SVM (Linear), (f) ANN, (j) Minimum distance, (h), ML, and (i) Mahalanobis.

Enhancing the spatial resolution of the LS dataset to 10 m (Fig. 6) results in significant improvements in OA for all classifiers ranging from 4.9% to 7.6%. The highest OA of 89.91% is achieved by utilizing the linear kernel of the SVM classifier. These findings are consistent with previous research reported by (Mateen *et al.*, 2023), who observed improved land cover classification OA by fusing Sentinel-2 and Landsat-8 images using a Gram-Schmidt algorithm. (Mansourmoghaddam *et al.*, 2022) also found that integrating Landsat 8 data with the 10 m Sentinel-2 bands can increase land cover classification accuracy by up to 10% compared to using the original Landsat 8 dataset. The improvement in separability is particularly notable for small-sized features such as branch roads, small resident units, bare lands between residents, and building shadows. The enhanced spatial resolution enables the classifiers to more effectively capture of the spectral signatures of these fine-grained features. This observation is consistent with the findings of (Sigurdsson *et al.*, 2022), who reported enhanced accuracy in classifying small features by fusing Landsat-8 and Sentinel-2 images using the S2Sharp approach. However, there were slight decreases in classification user's accuracies for larger-scale features, primarily due to false classifications occurring near the boundaries of these classes. These minor inaccuracies may be attributed to spectral distortions resulting from the pan-sharpening process. This notion is supported by the findings of (Al-Jasim *et al.*, 2022), who found that increasing in spatial resolution difference between merged images degrades the color quality of the resulting merged image.

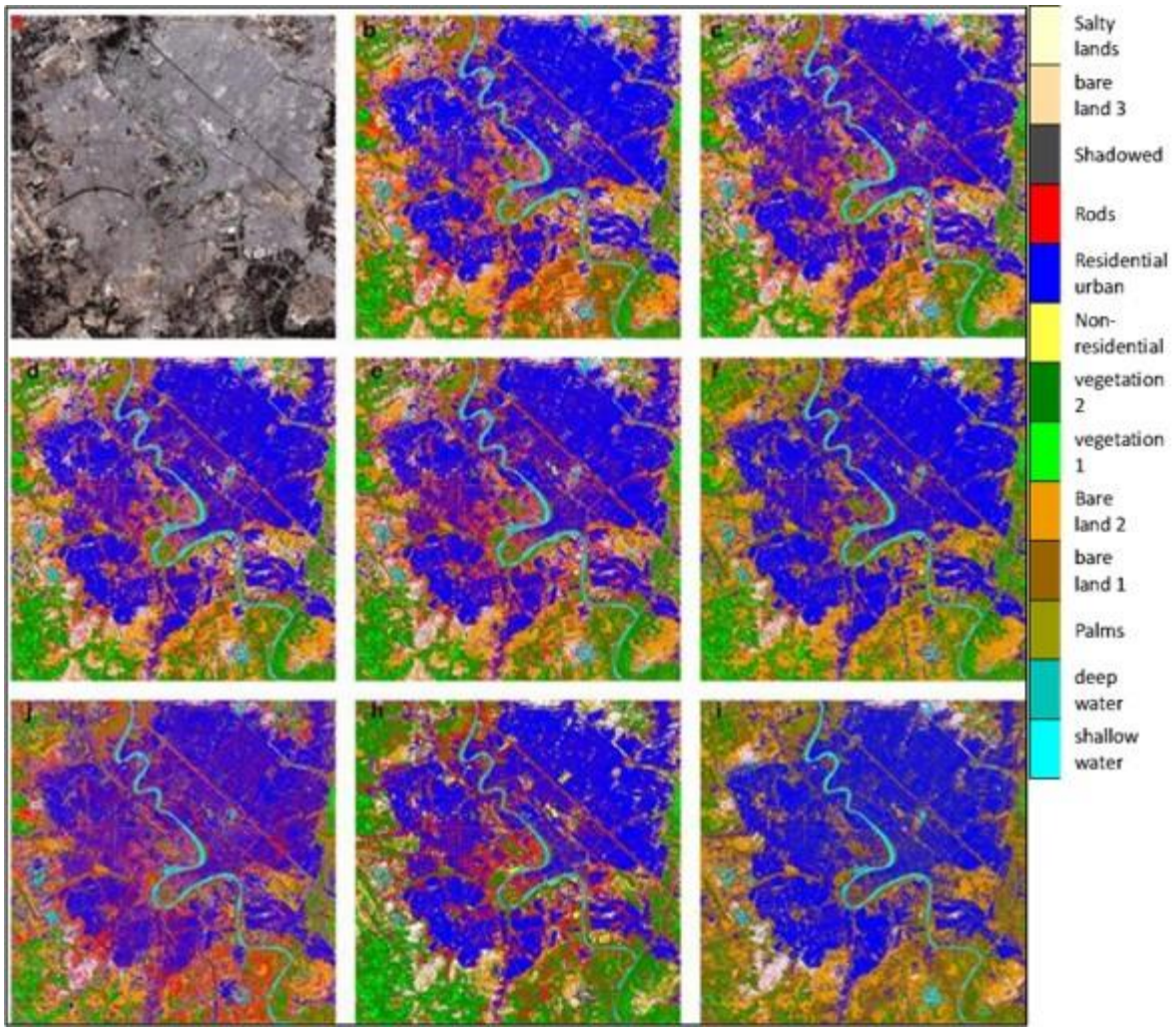

Fig. 6. Classification results of Landsat 10 m dataset; (a) Original image, (b) SVM (Sigmoid), (c) SVM (RBF), (d) SVM (Poly), (e) SVM (Linear), (f) ANN, (j) Minimum distance, (h), ML, and (i) Mahalanobis.

The (SENT 10 m) dataset (Fig. 7) is a fusion of data from Sentinel 2A, incorporating bands with different spatial resolutions (10, 20, and 60 m). These bands are pan-sharpened using the synthetic panchromatic band, resulting in a dataset with high spectral and spatial resolutions. The classification results demonstrate excellent overall accuracy (OA) across all classifiers. The linear kernel of the SVM classifier stands out as the top performer, achieving an OA of 92.42%, while the minimum distance classifier exhibited the lowest classification results at 83.06%.

This dataset's strength lies in its capability to offer valuable insights by leveraging a large number of well-registered bands (12 bands) to enhance the accuracy and comprehensiveness of classification results. All bands are accurately registered, meaning they have the same georeferenced information and field of view due to being acquired from the same platform. These results are consistent with the findings of Bouslihim et al. (2022), who attributed the superior performance of Sentinel-2 imagery to its high spatial resolution and a wider range of spectral bands compared to Landsat-9. The authors conclude that Sentinel-2 imagery outperformed Landsat-9 imagery in land cover classification using machine learning classifiers.

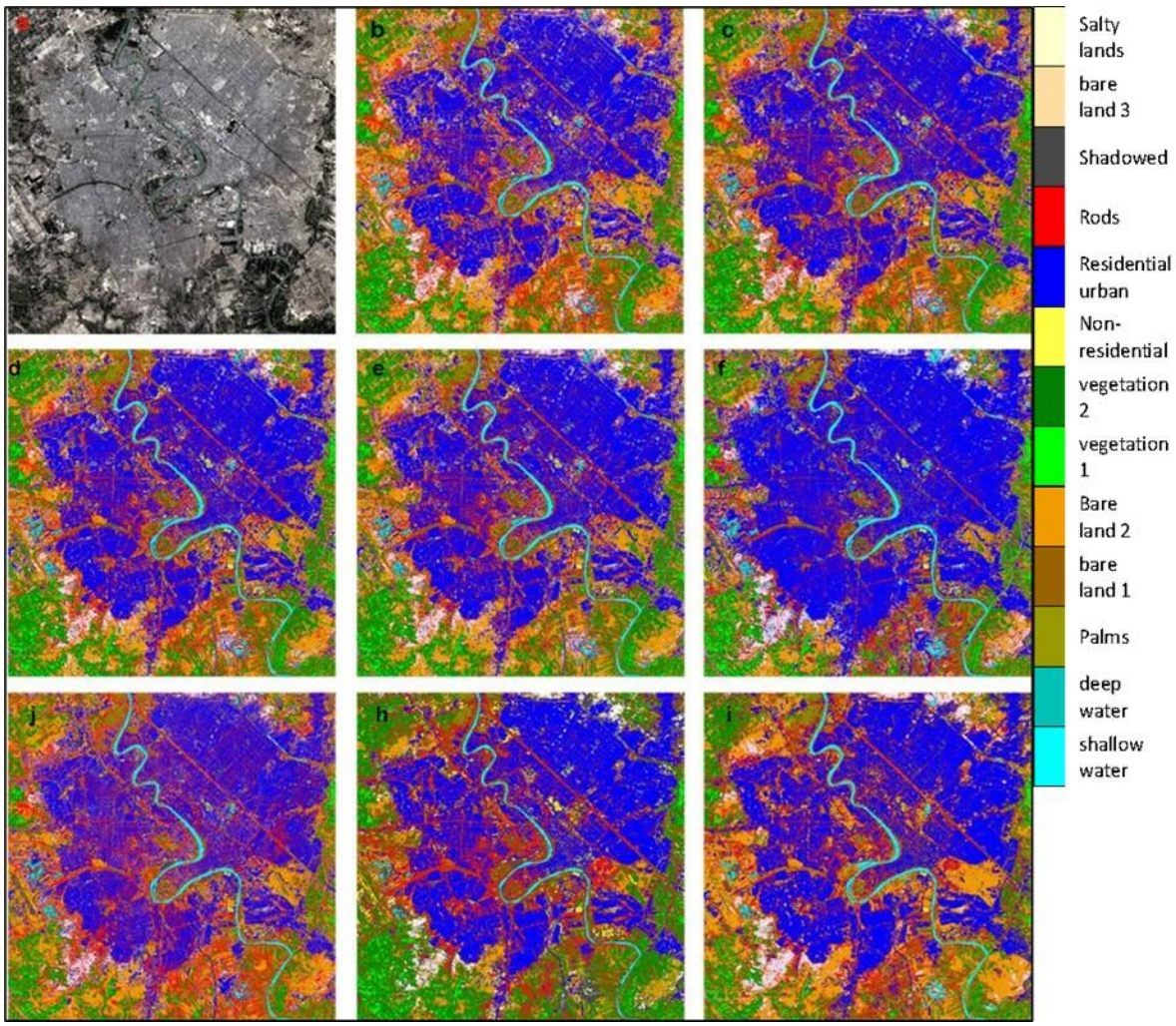

Fig. 7. Classification results of (SENT 10 m) dataset; (a) Original image, (b) SVM (Sigmoid), (c) SVM (RBF), (d) SVM (Poly), (e) SVM (Linear), (f) ANN, (j) Minimum distance, (h), ML, and (i) Mahalanobis.

Figure (8) illustrates the hybrid dataset resulting from the fusion of Sentinel 2A and Landsat 9 data highlighting the significance of data fusion. Through pan-sharpening, these datasets are harmonized, effectively combining their spatial and spectral attributes into a unified dataset. The classification accuracy of the hybrid dataset proves to be competitive, with the SVM classifier's linear kernel leading with an overall accuracy (OA) of 91.55% as indicated in Table (2) and Figure (10). This dataset does not only showcase the effectiveness of the SVM classifier but also demonstrates the potential benefits of synergistically integrating information from multiple sources. This comprehensive approach to data integration enables a deeper understanding of land cover dynamics, thus benefiting various geospatial applications.

Furthermore, the hybrid dataset successfully enhances the discrimination between spectrally overlapped classes like shadowed regions and water bodies as well as different types of vegetation regions. However, it is noted that improving co-registration between the original data sources could further enhance the classification results of this dataset. Authors such as (Ehlers *et al.*, 2010) and (Langheinrich, 2014) emphasize the importance of co-registration in data fusion since even minor misalignments can significantly degrade the quality of the fused image.

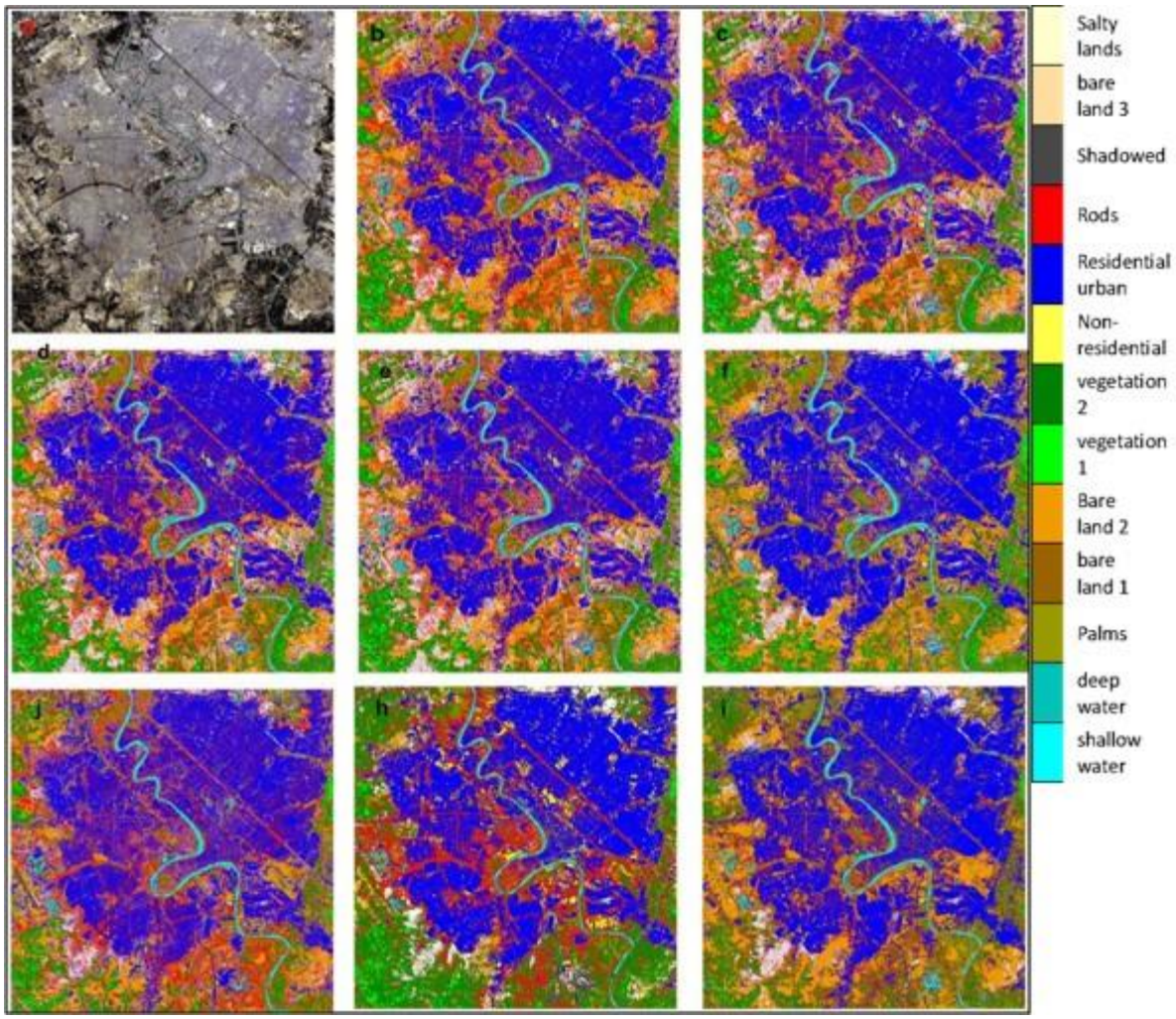

Fig. 8. Classification results of the (hybrid) dataset; (a) Original image, (b) SVM (Sigmoid), (c) SVM (RBF), (d) SVM (Poly), (e) SVM (Linear), (f) ANN, (j) Minimum distance, (h), ML, and (i) Mahalanobis.

The hybrid dataset significantly improves land cover classification accuracy, especially for sub-road extraction, small green regions, and palms. The hybrid dataset also reduces classification errors that can occur when using the original datasets individually such as the misclassification of waters as shadow areas. The classifier that deals with Sentinel data occasionally misclassifies waters as shadow areas. Figure (9) displays the improvement in the ability to distinguish and separate between various classes in different datasets for selected parts of the study site, particularly sub-road extraction, small green regions, and palms. As example, two samples are sharply contoured in the pan-sharpened dataset of (10 m) (d, e, and f), which are not clear in the dataset with (30, and 15) m (b and c), such as the boundaries of the People's Stadium which is located in the lower-left section (indicated by the yellow square), and the memorial structure (Martyr structure) in the upper central part of the clipped region (indicated by the black square).

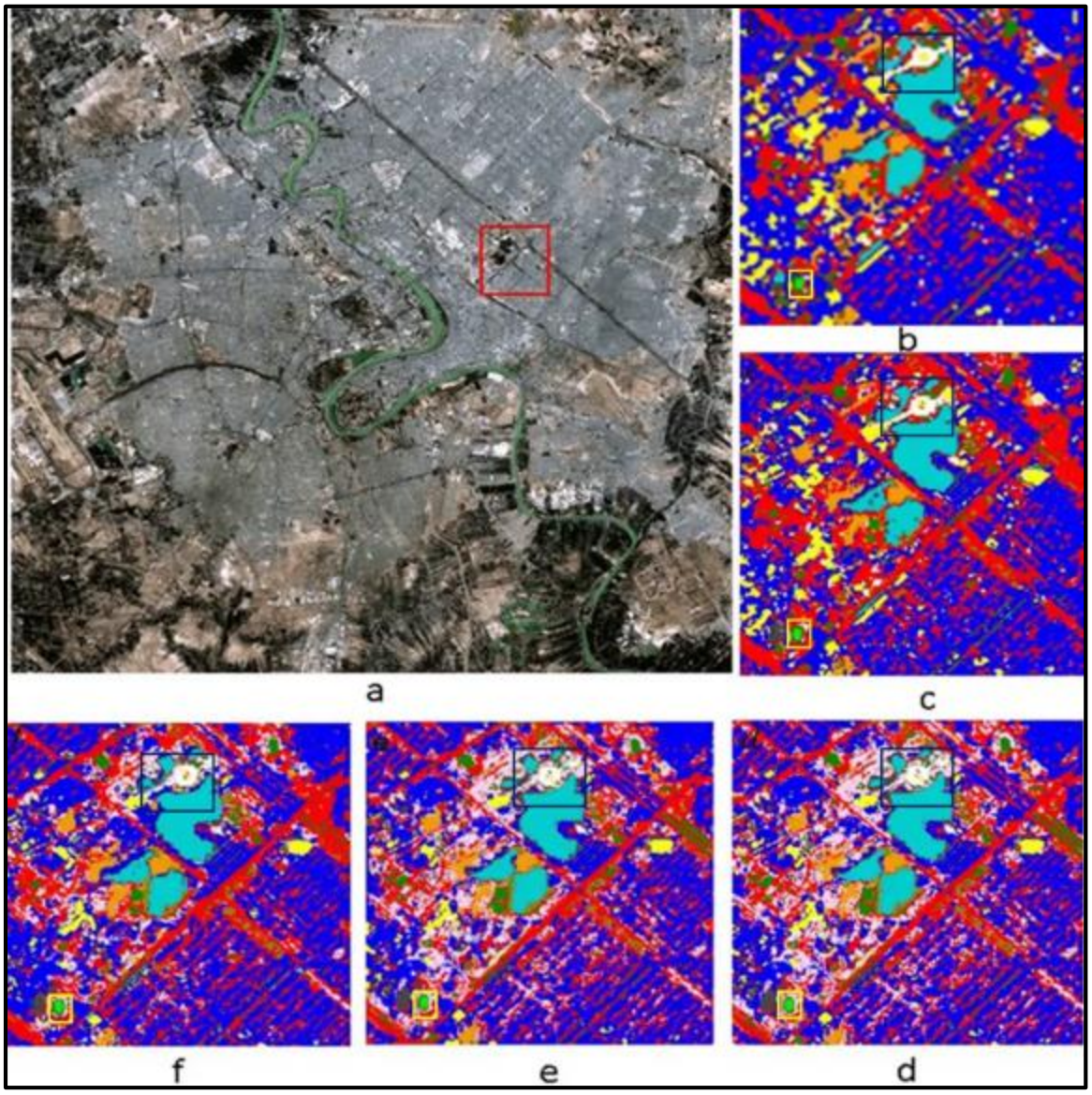

Fig. 9. (a) Sample area of the original dataset, (b) LS 30 m, (c) LS 15 m, (d) LS 10 m, (e) Sent 10 m, (f) hybrid 10 m) the classified dataset, to show the changes in classification accuracy for the selected area

The comprehensive results of this study as detailed in Table (2) and Figure (10) emphasize the effectiveness of pan-sharpening and data fusion techniques in enhancing spatial resolution and improving classification performance in remote sensing imagery. It's crucial to thoughtfully select the classifier and pan-sharpening algorithm considering the unique characteristics of the dataset and the context of the application.

This research illustrates the potential benefits of combining diverse remotely sensed data sources to enrich Earth observation applications. The hybrid dataset with its expanded range of available bands provides numerous band combinations facilitating the selection of training data and distinguishing between the classes with similar spectral signatures.

These findings offer valuable insights into the practicality and advantages of pan-sharpening techniques and data fusion in remote sensing applications promoting further exploration in this field. Researchers can utilize this information to effectively select the optimal band combination tailored to their specific remote sensing tasks.

However, it's important to acknowledge that minor co-registration mismatches between the original datasets can lead to some misclassifications in the study area. The quality of pan-sharpened satellite images decreases periodically and linearly with increasing co-registration

errors (Langheinrich, 2014). Differences in the fields of view between satellites, and potential distortion in spectral and spatial attributes of the fused data, may be a result of inherent limitations in the fusion algorithm (Mansourmoghaddam *et al.*, 2022; Rahimzadeganasl *et al.*, 2019). For land cover classification tasks, particularly when using pan-sharpened and fused imagery, the SVM's linear kernel is often a suitable choice. This is because the linear kernel is relatively straightforward and efficient to train, and it is adept at handling high-dimensional data. Moreover, the linear kernel is less susceptible to overfitting compared to other kernels, such as the RBF kernel (Bouslihim *et al.*, 2022).

Table 2: Overall accuracy percent of the different supervised classification algorithms

Data	Linear	Poly	RBF	Sigmoid	ML	ANN	Mahalanobis	Min distance
LS 30 m	82.28%	81.43%	81.46%	81.46%	78.82%	82.86%	74.13%	74.44%
LS 15 m	87.26%	86.26%	86.19%	84.10%	80.75%	81.22%	76.56%	79.14%
LS 10 m	89.91%	88.98%	88.96%	87.27%	82.77%	87.72%	80.09%	82.41%
SENT 10 m	92.42%	89.99%	89.99%	89.43%	86.68%	90.23%	83.75%	83.06%
hybrid	91.55%	89.40%	89.45%	88.11%	84.89%	88.51%	84.33%	83.00%

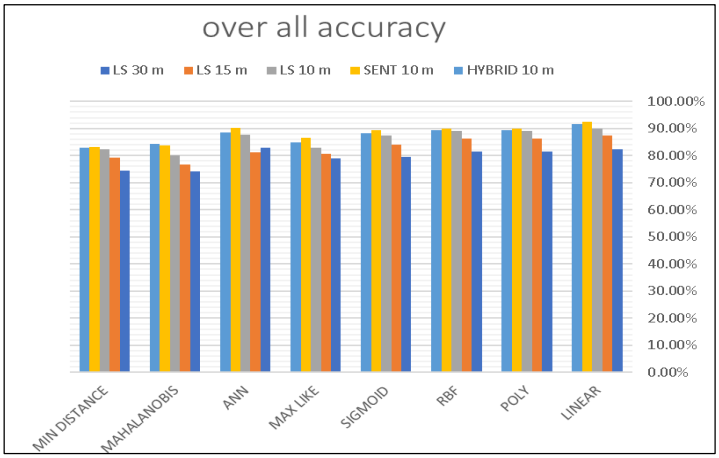

Fig. 10. Classification accuracy of the supervised classification algorithms.

Conclusions

This research evaluates how using pan-sharpened and fused data from Sentinel-2A and Landsat-9 satellites influences the precision of land use/land cover (LU/LC) classification. A panchromatic band is synthesized to enhance spatial resolution by averaging four bands with 10 m resolutions from the Sentinel-2 satellite. This synthesized band is then used in the pan-sharpening process for the remaining Sentinel-2 satellite bands (20 and 60 m) as well as for sharpening the Landsat-9 satellite bands (30 m). This increases the spatial resolution of both satellites to 10 m. The study finds that this increase in the spatial resolution significantly improves classification accuracy, especially when distinguishing features with small spatial dimensions compared to the original satellite resolutions. Furthermore, augmenting spectral resolution by integrating spectrally non-overlapping bands from both satellites into a hybrid dataset led to noticeable improvements in differentiating classes with overlapping spectral signatures. The study employed several supervised classification algorithms with the support vector machine (SVM) algorithm, particularly the linear kernel, yielding the highest result in most cases. This is because this kernel is less likely to overfit and can better generalize to unseen data. The study's findings have potential applications in various geospatial fields, such as urban planning, environmental monitoring, and disaster management. For instance, the enhanced classification accuracy achieved using composite data from multiple satellites could be used to create more detailed and informative land cover maps to aid decision-making processes in these areas.

To further improve generalization and minimize errors, future work could consider using another pan-sharpening algorithm such as a wavelet-based algorithm, and a larger number

of ground control points to reduce the error rate in joint registration. Additionally, fusing images from other satellites and study areas could further improve the generalization of the results.

Acknowledgments

The researcher would like to express gratitude to the supervisor Prof. Dr. Taghreed Abdulhameed Naji for her support and help in completing and carrying out this research work.

Conflict of Interest

The authors declare that there are no conflicts of interest regarding the publication of this manuscript

References

Abduljabbar, H. and Naji, T., 2020. Separating The Terrain Cover of Iraqi Marshes Region Using New Satellite Band Combination. The Iraqi Journal of Agricultural Science, 51(6), 1504-1516. https://doi.org/10.1088/1742-6596/1003/1/012083

Abduljabbar, H. M., 2017. Satellite Images Fusion Using Modified PCA Substitution Method. Ibn Al-Haitham Journal for Pure and Applied Sciences, 30(1), 29-37. https://doi.org/10.30526/30.1.1057

Abdullah, S. A., Abbas, K. H., Harif, A. H., Alaa, R. F. and Hiba, S., 2023. Sustainable Urban Distribution of Educational Institutions and Population Density in Baghdad City Using Remote Sensing Techniques. IOP Conference Series: Earth and Environmental Science, 1202(1), 012015. https://doi.org/10.1088/1755-1315/1202/1/012015

Aguilera, M. A. Z., 2020. Classification Of Land-Cover Through Machine Learning Algorithms For Fusion Of Sentinel-2a And Planetscope Imagery. 2020 IEEE Latin American GRSS and ISPRS Remote Sensing Conference (LAGIRS),

Ahmad, A. and Quegan, S., 2012. Analysis of maximum likelihood classification technique on Landsat 5 TM satellite data of tropical land covers. 2012 IEEE International Conference on Control System, Computing and Engineering,

Akula, R., Gupta, R. and Devi, M. V., 2012. An efficient PAN sharpening technique by merging two hybrid approaches. Procedia Engineering, 30, 535-541. https://doi.org/10.1016/j.proeng.2012.01.895

Al-Jasim, A. A. N., Naji, T. A. and Shaban, A. H., 2022. The Effect of Using the Different Satellite Spatial Resolution on the Fusion Technique. Iraqi Journal of Science, 4131-4141. https://doi.org/10.24996/ijs.2022.63.9.40

Al-Rubiey, I. J., 2017. Increase the intelligibility of multispectral image using pan-sharpening techniques for many remotely sensed images. Ibn Al-Haitham Journal For Pure and Applied Sciences, 28(3).

Ali, Z. R. and Muhaimeed, A. S., 2016. The study of temporal changes on land cover/land use prevailing in Baghdad governorate using RS and GIS. The Iraqi Journal of Agricultural Sciences, 47(3), 846-855. https://doi.org/10.36103/ijas.v47i3.576

Amro, I., Mateos, J., Vega, M., Molina, R. and Katsaggelos, A. K., 2011. A survey of classical methods and new trends in pansharpening of multispectral images. EURASIP Journal on Advances in Signal Processing, 2011(1), 1-22. https://doi.org/10.1186/1687-6180-2011-79

Bouslihim, Y., Kharrou, M. H., Miftah, A., Attou, T., Bouchaou, L. and Chehbouni, A., 2022. Comparing pan-sharpened landsat-9 and sentinel-2 for land-use classification using

machine learning classifiers. Journal of Geovisualization and Spatial Analysis, 6(2), 35. https://doi.org/10.1007/s41651-022-00130-0

Canty, M. J., 2019. Image analysis, classification and change detection in remote sensing: with algorithms for ENVI/IDL and Python (Fourth edition ed.). Crc Press. https://doi.org/10.1201/9780429464348

Choate, M. J., Rengarajan, R., Storey, J. C. and Lubke, M., 2022. Landsat 9 Geometric Characteristics Using Underfly Data. Remote Sensing, 14(15), 3781. https://doi.org/10.3390/rs14153781

Drakonakis, G. I., Tsagkatakis, G., Fotiadou, K. and Tsakalides, P., 2022. OmbriaNet—supervised flood mapping via convolutional neural networks using multitemporal sentinel-1 and sentinel-2 data fusion. IEEE Journal of selected topics in applied earth observations and remote sensing, 15, 2341-2356. https://doi.org/10.1109/JSTARS.2022.3155559

Ehlers, M., Klonus, S., Johan Åstrand, P. and Rosso, P., 2010. Multi-sensor image fusion for pansharpening in remote sensing. International Journal of Image and Data Fusion, 1(1), 25-45. https://doi.org/10.1080/19479830903561985

ESA, E., 2015. Sentinel-2 user handbook. Sentinel-2 User Handbook, 64.

ESA, V. B., Szantoi, Z., and Gascon, F., 2020. Copernicus Sentinel-2 Mission: Calibration and Validation activities. GSICS Q, 14(1). https://doi.org/10.1080/22797254.2019.1582840

Ghassemian, H., 2016. A review of remote sensing image fusion methods. Information Fusion, 32, 75-89. https://doi.org/10.1016/j.inffus.2016.03.003

Giri, C. P., 2012. Remote sensing of land use and land cover: principles and applications (1st Edition ed.). CRC press. https://doi.org/10.1201/b11964

Hafner, S., Nascetti, A., Azizpour, H. and Ban, Y., 2021. Sentinel-1 and sentinel-2 data fusion for urban change detection using a dual stream u-net. IEEE Geoscience and Remote Sensing Letters, 19, 1-5. https://doi.org/10.1109/LGRS.2021.3119856

Hatem, A. J., Al-Jasim, A. A. N. and Abduljabbar, H. M., 2021. A study of the climate and human impact on the future survival of the Al-Sannya marsh in Iraq. Journal of Water and Land Development, 168-173-168-173. https://doi.org/10.24425/jwld.2021.139027

Hogland, J., Billor, N. and Anderson, N., 2013. Comparison of standard maximum likelihood classification and polytomous logistic regression used in remote sensing. European Journal of Remote Sensing, 46(1), 623-640. https://doi.org/10.5721/EuJRS20134637

Kaplan, G. and Avdan, U., 2018. Sentinel-2 pan sharpening—comparative analysis. Proceedings,

Klonus, S. and Ehlers, M., 2009, July 6-9, 2009. Performance of evaluation methods in image fusion. 2009 12th International Conference on Information Fusion, Seattle, WA, USA.

Laben, C. A. and Brower, B. V., 2000. Process for enhancing the spatial resolution of multispectral imagery using pan-sharpening. In: Google Patents.

Lambin, E. F. and Geist, H. J., 2008. Land-use and land-cover change: local processes and global impacts. Springer Science and Business Media. https://doi.org/10.1007/3-540-32202-7

Langheinrich, M., 2014. On the influence of coregistration errors on satellite image pansharpening methods Hochschule für Angewandte Wissenschaften München].

Liu, X., He, J., Yao, Y., Zhang, J., Liang, H., Wang, H., and Hong, Y. (2017). Classifying urban land use by integrating remote sensing and social media data. International Journal of

Geographical Information Science, 31(8), 1675-1696. https://doi.org/10.1080/13658816.2017.1324976

Maciel, D. A., Pahlevan, N., Barbosa, C. C. F., de Novo, E. M. L. d. M., Paulino, R. S., Martins, V. S., . . . Crawford, C. J., 2023. Validity of the Landsat surface reflectance archive for aquatic science: Implications for cloud-based analysis. Limnology and Oceanography Letters, 8(6), 850-858. https://doi.org/10.1002/lol2.10344

Majed, M. A. and Abduljabbar, H. M., 2022. The Change in the Land Cover of Mahmudiyah City in Iraq for the Last Three Decades. Ibn Al-Haitham Journal For Pure and Applied Sciences, 35(3). https://doi.org/10.30526/35.3.2831

Mansourmoghaddam, M., Rousta, I., Ghaffarian, H. and Mokhtari, M. H., 2022. Evaluating the capability of spatial and spectral fusion in land-cover mapping enhancement. Earth Observation and Geomatics Engineering, 6(1), -. https://doi.org/10.22059/eoge.2022.348987.1125

Masek, J. G., Wulder, M. A., Markham, B., McCorkel, J., Crawford, C. J., Storey, J. and Jenstrom, D. T. 2020. Landsat 9: Empowering open science and applications through continuity. Remote Sensing of Environment, 248, 111968. https://doi.org/10.1016/j.rse.2020.111968

Mateen, S., Nuthammachot, N., Techato, K. and Ullah, N., 2023. Billion Tree Tsunami Forests Classification Using Image Fusion Technique and Random Forest Classifier Applied to Sentinel-2 and Landsat-8 Images: A Case Study of Garhi Chandan Pakistan. ISPRS International Journal of Geo-Information, 12(1), 9. https://doi.org/10.3390/ijgi12010009

Maurer, T., 2013. How to pan-sharpen images using the gram-schmidt pan-sharpen method–A recipe. Int. Arch. Photogramm. Remote Sens. Spatial Inf. Sci. https://doi.org/10.5194/isprsarchives-XL-1-W1-239-2013

Micijevic, E., Barsi, J., Haque, M. O., Levy, R., Anderson, C., Thome, K., . . . Helder, D., 2022. Radiometric performance of the Landsat 9 Operational Land Imager over the first 8 months on orbit (Vol. 12232). SPIE. https://doi.org/10.1117/12.2634301

Mountrakis, G., Im, J. and Ogole, C., 2011. Support vector machines in remote sensing: A review. ISPRS Journal of Photogrammetry and Remote Sensing, 66(3), 247-259. https://doi.org/10.1016/j.isprsjprs.2010.11.001

Muhsin, I. J. and Foud, K. M., 2012. Improving spatial resolution of satellite image using data fusion method. Iraqi Journal of Science, 53(4), 943-949. https://doi.org/ 10.24996/ijs.2022.63.9.40

Muhsin, I. J. and Salih, K. H., 2015. Enhancement and Quality Assessment of Multi-Spectral Image Using Different Fusion Methods. Iraqi Journal of Science, 56(1A), 257-264.

Murtaza, K. O. and Romshoo, S. A., 2014. Assessing the impact of spatial resolution on the accuracy of land cover classification. Journal of Himalayan Ecology and Sustainable Development, 9.

Naji, T. A., 2018. Study of vegetation cover distribution using DVI, PVI, WDVI indices with 2D-space plot. Journal of Physics: conference series, 1003, 012083. https://doi.org/10.1088/1742-6596/1003/1/012083

Naji, T. A. and Hatem, A. J., 2017. New adaptive satellite image classification technique for al Habbinya region west of Iraq. Ibn Al-Haitham Journal For Pure and Applied Sciences, 26(2), 143-149.

Niroumand-Jadidi, M., Bovolo, F., Bresciani, M., Gege, P. and Giardino, C., 2022. Water Quality Retrieval from Landsat-9 (OLI-2) Imagery and Comparison to Sentinel-2. Remote Sensing, 14(18), 4596. https://doi.org/10.3390/rs14184596

Pham, T. D., Xia, J., Ha, N. T., Bui, D. T., Le, N. N. and Takeuchi, W., 2019. A review of remote sensing approaches for monitoring blue carbon ecosystems: Mangroves, seagrasses and salt marshes during 2010–2018. Sensors, 19(8), 1933. https://doi.org/10.3390/s19081933

Pohl, C. and Van Genderen, J., 2016. Remote sensing image fusion: A practical guide. Crc Press. https://doi.org/10.1201/9781315370101

Raheem, M. A. and Hatem, A. J., 2019. Calculation of Salinity and Soil Moisture indices in south of Iraq-Using Satellite Image Data. Energy Procedia, 157, 228-233. https://doi.org/10.1016/j.egypro.2018.11.185

Rahimzadeganasl, A., Alganci, U. and Goksel, C., 2019. An Approach for the Pan Sharpening of Very High-Resolution Satellite Images Using a CIELab Color Based Component Substitution Algorithm. Applied Sciences, 9(23), 5234. https://doi.org/10.3390/app9235234

Rahman, M. M. and Robson, A., 2020. Integrating Landsat-8 and Sentinel-2 Time Series Data for Yield Prediction of Sugarcane Crops at the Block Level. Remote Sensing, 12(8), 1313. https://doi.org/10.3390/rs12081313

Roth, K. L., Roberts, D. A., Dennison, P. E., Peterson, S. H. and Alonzo, M., 2015. The impact of spatial resolution on the classification of plant species and functional types within imaging spectrometer data. Remote Sensing of Environment, 171, 45-57. https://doi.org/10.1016/j.rse.2015.10.004

Saleh, S. A., 2010. Impact of urban expansion on surface temperature Inbaghdad, Iraq using remote sensing and GIS techniques. Al-Nahrain Journal of Science, 13(1), 48-59. https://doi.org/10.22401/JNUS.13.1.07

Sigurdsson, J., Armannsson, S. E., Ulfarsson, M. O. and Sveinsson, J. R., 2022. Fusing sentinel-2 and landsat 8 satellite images using a model-based method. Remote Sensing, 14(13), 3224. https://doi.org/10.3390/rs14133224

Toure, S. I., Stow, D. A., Shih, H.-c., Weeks, J. and Lopez-Carr, D., 2018. Land cover and land use change analysis using multi-spatial resolution data and object-based image analysis. Remote Sensing of Environment, 210, 259-268. https://doi.org/10.1016/j.rse.2018.03.023

Townshend, J. R., Justice, C. O., Gurney, C. and McManus, J., 1992. The impact of misregistration on change detection. IEEE transactions on geoscience and remote sensing, 30(5), 1054-1060. https://doi.org/10.1109/36.175340

Vivone, G., Alparone, L., Chanussot, J., Dalla Mura, M., Garzelli, A., Licciardi, G. A., Wald, L., 2014. A critical comparison among pansharpening algorithms. IEEE transactions on geoscience and remote sensing, 53(5), 2565-2586. https://doi.org/10.1109/TGRS.2014.2361734

Waldner, F., Fritz, S., Di Gregorio, A. and Defourny, P., 2015. Mapping priorities to focus cropland mapping activities: Fitness assessment of existing global, regional and national cropland maps. Remote Sensing, 7(6), 7959-7986. https://doi.org/10.3390/rs70607959

Wang, Q., Blackburn, G. A., Onojeghuo, A. O., Dash, J., Zhou, L., Zhang, Y. and Atkinson, P. M., 2017. Fusion of Landsat 8 OLI and Sentinel-2 MSI Data. IEEE transactions on geoscience and remote sensing, 55(7), 3885-3899. https://doi.org/10.1109/TGRS.2017.2683444

Wang, Q., Shi, W., Li, Z. and Atkinson, P. M., 2016. Fusion of Sentinel-2 images. Remote Sensing of Environment, 187, 241-252. https://doi.org/10.1016/j.rse.2016.10.030

Weng, W.-D., Yang, C.-S. and Lin, R.-C., 2007. A channel equalizer using reduced decision feedback Chebyshev functional link artificial neural networks. Information Sciences, 177(13), 2642-2654. https://doi.org/10.1016/j.ins.2007.01.006

Wulder, M. A., Roy, D. P., Radeloff, V. C., Loveland, T. R., Anderson, M. C., Johnson, D. M., . . . Pahlevan, N., 2022. Fifty years of Landsat science and impacts. Remote Sensing of Environment, 280, 113195. https://doi.org/10.1016/j.rse.2022.113195